The Journal of Adhesion
Publication details, including instructions for authors and subscription information:
http://www.tandfonline.com/loi/gadh20

Adhesion of Flat and Structured PDMS Samples to Spherical and Flat Probes: A Comparative Study

Elmar Kroner [a], Dadhichi R. Paretkar [a], Robert M. McMeeking [a b] & Eduard Arzt [a]

[a] INM - Leibniz Institute for New Materials, Functional Surfaces Group, Saarbrücken, Germany

[b] Department of Mechanical Engineering, University of California, Santa Barbara, CA, USA

Published online: 25 May 2011.

To cite this article: Elmar Kroner, Dadhichi R. Paretkar, Robert M. McMeeking & Eduard Arzt (2011) Adhesion of Flat and Structured PDMS Samples to Spherical and Flat Probes: A Comparative Study, The Journal of Adhesion, 87:5, 447-465, DOI: 10.1080/00218464.2011.575317

To link to this article: http://dx.doi.org/10.1080/00218464.2011.575317

The Journal of Adhesion, 87:447–465, 2011

ISSN: 0021-8464 print/1545-5823 online
DOI: 10.1080/00218464.2011.575317

Taylor & Francis
Taylor & Francis Group

Adhesion of Flat and Structured PDMS Samples to Spherical and Flat Probes: A Comparative Study

Elmar Kroner[1], Dadhichi R. Paretkar[1], Robert M. McMeeking[1,2], and Eduard Arzt[1]
[1]INM – Leibniz Institute for New Materials, Functional Surfaces Group, Saarbrücken, Germany
[2]Department of Mechanical Engineering, University of California, Santa Barbara, CA, USA

Adhesion measurements on poly(dimethyl)siloxane samples were performed, for the first time, with flat glass probes under controlled tilt angle and the results were compared with measurements from spherical probes of two different radii. Experiments were made on both flat and patterned samples with structure diameters of 4.7 μm and heights of 0.82 μm and 1.95 μm, respectively. Pull-off forces measured with spherical probes showed the usual preload dependence and were independent of misalignment angle. On the other hand, pull-off forces measured with aligned flat probes were preload-independent, but dropped significantly and became preload-dependent with increasing misalignment. This effect was more pronounced for structured samples, where a misalignment by 0.2° resulted in a drop of adhesion by more than 30%. The comparison indicates that measurements from spherical probes underestimate adhesive forces for structured surfaces if compared with aligned flat probes. Finally, we propose a simple model which allows the prediction of angle-dependent plateau values of pull-off forces for measurements with flat probes on flat samples.

Keywords: Adhesion; Bioinspired; Biomimetic; Fibrillar surfaces; Gecko; Pull-off

1. INTRODUCTION

Intense investigation of biomimetic adhesives has occurred over the last several years. Surface structures of increasing complexity have

Received 22 September 2010; in final form 25 January 2011.

One of a Collection of papers honoring Chung-Yuen Hui, the recipient in February 2011, of *the Adhesion Society Award for Excellence in Adhesion Science, Sponsored by 3M*.

Address correspondence to Elmar Kroner, INM – Leibniz Institute for New Materials, Functional Surfaces Group, Campus D2 2, D-66123, Saarbrucken, Germany. E-mail: elmar.kroner@inm-gmbh.de

been fabricated, such as simple cylindrical pillar structures [1–5], hierarchical structures [6–11], and structures with defined tilt angles [8,12–14] and different tip shapes [10,13–22]. Besides measurements of friction [3,8–9,14,23] or frictional adhesion [22], the most common method for determining normal adhesion is the so-called JKR-type experiment [1–2,4,6,10–13,18–20,24–25], named after Johnson, Kendall and Roberts [26]. In their original work, two soft elastic spheres were brought into contact and area of contact as well as pull-off force were measured [27,28]. The results led to the now well known JKR theory [26] for contact between soft spheres. For practical reasons, the experimental setup nowadays often consists of a hard, spherical probe pressed against a soft, flat sample, and preload and pull-off force are measured [2,10,13,18].

Measurements with spherical probes are insensitive to misalignment and have been investigated theoretically [29–36]; data interpretation, however, has several problems. One of the main drawbacks is the increase of the contact area with increasing compressive preload, which complicates the determination of the pull-off strength. With regard to adhesion of structured surfaces, additional problems are encountered. For example, the stress state of individual pillars depends on their position within the contact area: while pillars in the contact boundary region are under tension during pull-off, pillars directly below the center of the probe may still be under compression. This leads to a stepwise detachment of structures [1,6,10,14], which will influence pull-off force values. A possible way to avoid such problems is to measure adhesion with a stiff flat probe against a larger flat, compliant sample [5]. The contact area is then constant and defined by the probe dimensions. Apart from a small region at the probe boundary, a uniform stress within the sample can be achieved. In contrast to experiments with spherical probes, the use of flat probes allows direct determination of the pull-off strength by simple division of the pull-off force by the area of the probe. However, adhesion measurements with a flat probe require careful parallel alignment of probe and sample to ensure reproducibility of data.

In this paper we present, for the first time, normal adhesion measurements from flat probes under controlled tilt angle, both on flat and structured samples. The results of these measurements are compared with adhesion data from spherical probes of two different radii. We then propose a model which predicts the angle dependence of the pull-off force plateau at high preload for measurements from flat probes on flat samples.

2. EXPERIMENTAL

2.1. Sample Preparation

Polydimethylsiloxane (PDMS) samples with a hexagonal array of pillars were fabricated in three process steps: photo lithography, reactive ion etching and two-step soft molding. For photo lithography, silicon wafers (Crystec GmbH, Altötting, Germany) were spin-coated with the photo resist SU 8-2 (MicroChem, Newton, MA, USA) to form a layer of 2 μm thickness. After exposure through a lithography mask (ML&C Jena GmbH, Jena, Germany) and treatment of the resist with a developer (mrdev-600, MicroChem) cylindrical structures were obtained.

To improve durability and cleanability of the templates, the pre-structured wafers were etched in a reactive ion etcher using a gas chopping protocol with SF_6 and CHF_3 as etching gases and CHF_3 as passivation gas. The remaining photo resist was stripped off by heating the wafers up to 600°C in air. Silicon cylinders were obtained, with structure heights being a function of the etching time.

The silicon wafers were then used as a mold. Two molding steps were necessary to obtain cylindrical polymer structures. The first molding was performed with polyurethane (PU) (PolyOptic 1470, PolyConForm GmbH, Düsseldorf, Germany). After cross-linking at room temperature for 48 hours, the PU was peeled off the wafers resulting in polymer molds with cylindrical holes. In the second step, the PU molds were used to fabricate PDMS samples with cylindrical structures. Sylgard 184 PDMS (Dow Corning, Barry, Wales, UK) was mixed in a 10:1 (pre-polymer to cross-linker) ratio. After removal of air bubbles formed during mixing in vacuum, the viscous liquid was poured onto the PU template and cross-linked at 75°C for 72 hours. After cross-linking, the PDMS samples were peeled off the PU template resulting in structured PDMS samples. Flat PDMS samples were prepared under identical conditions and were used as a control.

2.2. Adhesion Measurements

Adhesion measurements were performed on a custom-built apparatus known as the Macroscopic Adhesion measurement Device (MAD), as previously described [37,38]. Figure 1 shows a schematic of the adhesion tester. A 3-axis piezo stage (PI, Karlsruhe, Germany) was mounted to a 6-axis positioning table (PI, Karlsruhe, Germany) for high positioning and measurement accuracy. Forces were measured

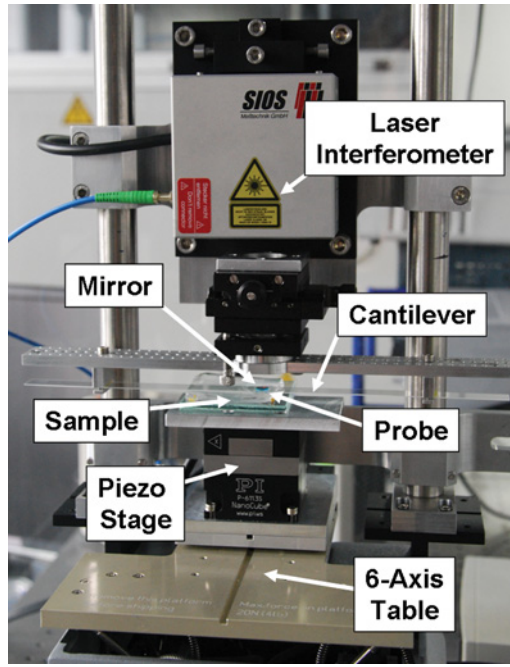

FIGURE 1 Setup of the adhesion tester MAD. The sample is brought into contact with the probe (glued to the cantilever) using a piezo and a 6-axis table. The latter allows high precision tilting. The deflection of the cantilever is continuously measured by laser interferometry. Forces are calculated from the cantilever deflection (color figure available online).

using a calibrated symmetric glass cantilever with tilt-free deflection up to several hundred micrometers. A mirror and the probe were glued to the top and the bottom of the cantilever, respectively. The cantilever deflection was measured using a laser interferometer (SIOS Messtechnik GmbH, Illmenau, Germany). The interferometer is very sensitive to tilt of the mirror and halts measurement if misalignment exceeds 2 arc minutes. Therefore, the intensity of the reflected laser beam served as an indirect control of cantilever tilt.

The sample was pressed against the probe with a defined preload and retracted in a standard load-displacement experiment. The pull-off force was defined as the maximum tensile force. Three different probes were used for adhesion measurements; two borosilicate glass spheres with 2 mm and 5 mm radius and a borosilicate glass flat-ended cylindrical probe having a diameter of 1 mm (peak to valley roughness $<$15 nm). All adhesion tests were performed at a velocity of

5 μm/s. The probes were cleaned with ethanol and brought into contact with a PDMS piece 1000 times before starting the measurements to ensure an equilibrium surface state of the probe [37].

To investigate misalignment effects, the samples tested with the flat probe had to be carefully aligned. Adhesion measurements were performed for different tilt angles at an accuracy of 0.02° in two axes, resulting in a point symmetric pull-off force profile map. The center of the symmetric profile was defined as 0° misalignment. The alignment was then systematically varied from −2° up to +2° in 0.2° steps. Measurements were also performed with spherical probes within ±2° tilt angle, although a definition of 0° misalignment was not possible in this case.

3. RESULTS

3.1. Sample Shape

The structured PDMS samples were characterized using white light interferometry. The samples consisted of cylindrical structures with $4.7 \pm 0.1\,\mu m$ diameter and heights of $0.82 \pm 0.02\,\mu m$ (referred to as AR0.2) and $1.95 \pm 0.02\,\mu m$ (referred to as AR0.4), respectively. These low aspect ratios were chosen to prevent structure buckling during loading. The structures were hexagonally packed with a center-to-center spacing of 10 μm, resulting in a packing density of 20.0%. The sample thickness was ∼880 μm. The structures were slightly conical and featured sharp edges. Fig. 2a and b show a cross section of an

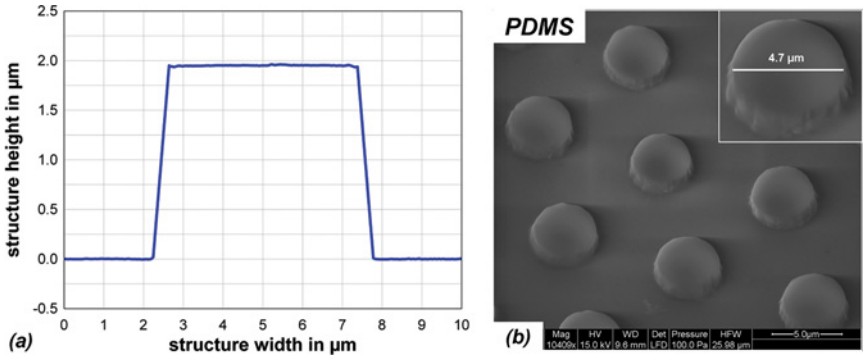

FIGURE 2 Geometry of the structures with a height of 1.95 μm and 4.7 μm diameter. In (a) a cross section measured by white light interferometry of a single structure is plotted. A SEM image is shown in (b) (color figure available online).

AR0.4 structure measured by white light interferometry and a SEM picture, respectively.

3.2. Angle Dependent Adhesion Using a Flat Probe

Adhesion measurements with the flat probe showed a strong dependence of pull-off forces on the tilt angle as shown in Fig. 3. For measurements in the aligned state, low or no dependence of pull-off force on preload was found for both flat and structured samples. With increasing tilt angle of the probe, the pull-off force values dropped significantly and became preload dependent. In the case of flat PDMS, a 0.2° tilt angle had a negligible preload dependence of the pull-off force but the value of the pull-off force was reduced by ~10% compared with

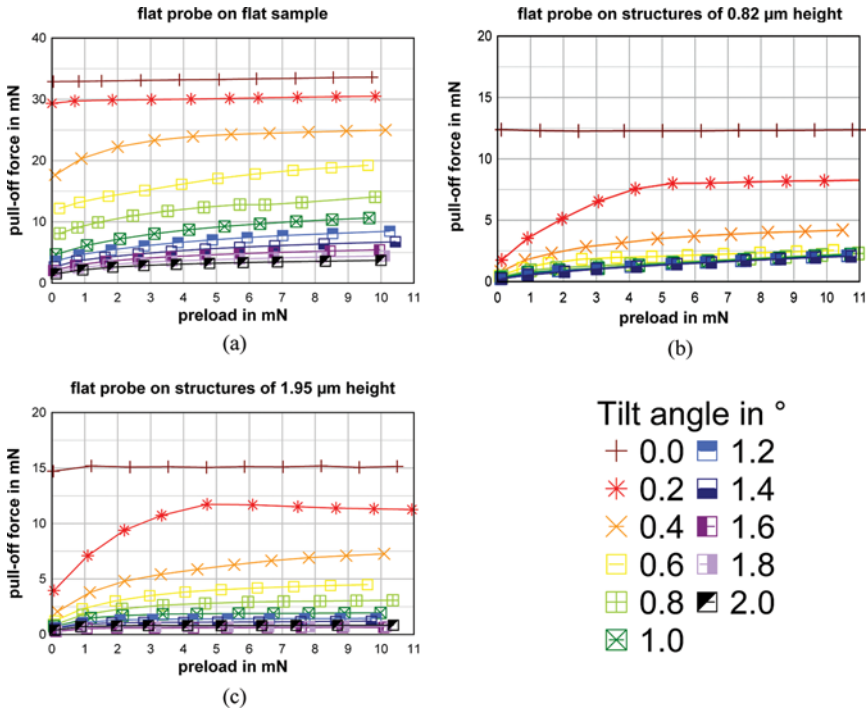

FIGURE 3 Adhesion measurements performed with a flat-ended cylindrical glass probe of 1 mm diameter at different misalignment angles. Angle scans were performed for (a) flat, (b) structured PDMS samples with a diameter of ~4.7 µm and heights of ~0.82 µm (AR0.2), and (c) structures of heights of ~1.95 µm (AR0.4) (color figure available online).

aligned measurements (Figure 3a). For a misalignment of 0.4°, the pull-off force showed an increased preload dependence. The pull-off force reached ~53% for low and ~74% for maximum preload, compared with aligned measurements. For a misalignment of 2.0°, the pull-off force showed a pronounced preload dependence and constituted less than ~10% of the force measured in the aligned state.

The preload and angle dependences of the pull-off force for structured samples are shown in Fig. 3b and 3c. For both aspect ratios the pull-off force dependence on misalignment was higher than for the flat control sample. A misalignment of 0.2° was sufficient to result in significant preload dependence. Compared with the force values obtained from aligned measurements, the pull-off forces measured on AR0.2 structures reached between 16% for low and 64% for high preload (Fig. 3b). For misalignment >0.6° the pull-off force did not

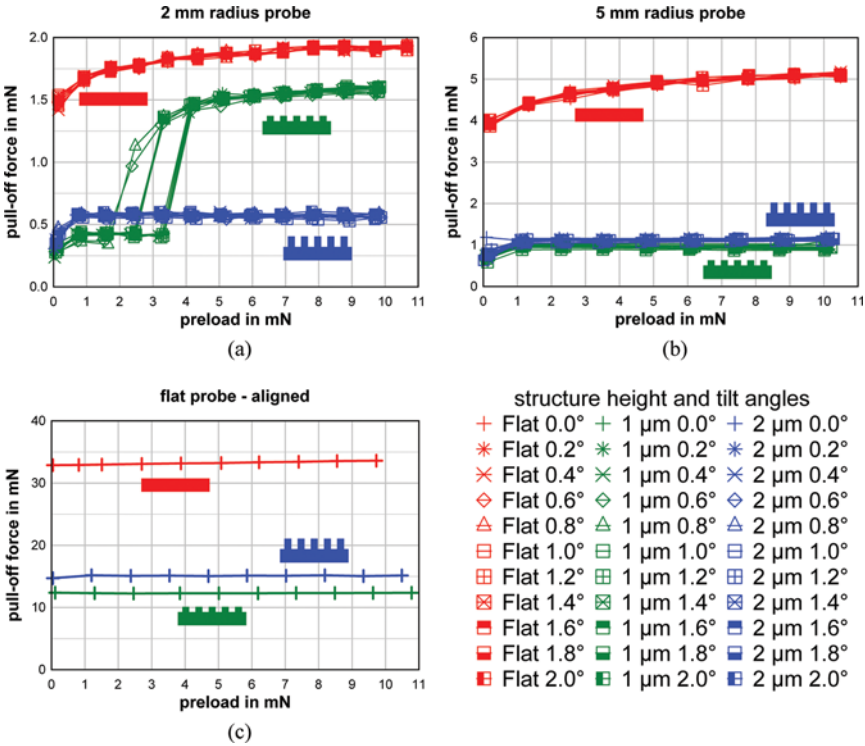

FIGURE 4 Adhesion measurements on flat and structured samples, performed with spherical probes of (a) 2 mm, (b) 5 mm radius, and (c) with a flat-ended cylindrical probe of 1 mm diameter in the aligned state (color figure available online).

change further with increasing tilt angle. For AR0.4 structures the pull-off force showed a similar dependence on misalignment as for the AR0.2 structure sample, but was less pronounced (Fig. 3c). A misalignment of 0.2° resulted in pull-off forces between 26% for the low and 80% for maximum preload compared with the value obtained from aligned measurements. In general, the pull-off forces for structured samples were lower than those for flat control samples, as the structures had relatively large diameters, a low aspect ratio and no adhesion enhancing tip geometry [2,18].

3.3. Comparison Between Different Probe Geometries

Figures 4a and b show the results of adhesion measurements from spherical probes (2 mm and 5 mm radii) on flat and structured PDMS

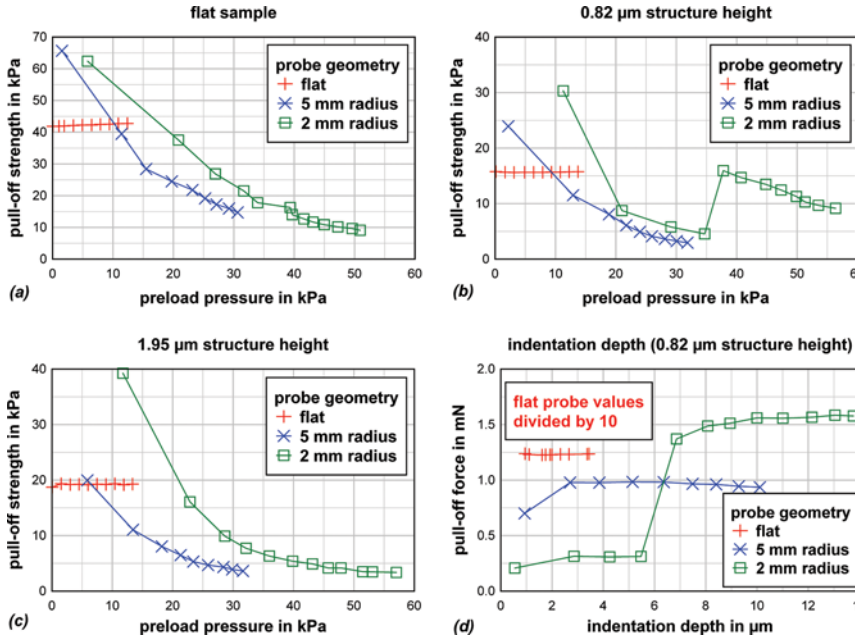

FIGURE 5 Representative adhesion strength curves, where the pull-off force from Figure 4 has been normalized by the projected contact area, calculated from the indentation depth and the probe geometry. Preload pressure and pull-off strength is shown for (a) the flat control sample and for, (b) the samples with structure diameters of ~4.7 µm and heights of ~0.82 µm, (c) heights of ~1.95 µm and (d) shows the indentation depth for the AR0.2 structure sample (color figure available online).

for different tilt angles. For these measurements, the tilt angle had no effect on the pull-off force. However, for the 2 mm radius probe a sudden increase in pull-off force was measured for AR0.2 structures at a preload of ~3 mN (Fig. 4a, green curve). Figure 4c shows the results for aligned measurements with a flat probe. Additional measurement graphs are shown in Supporting Information.

Figures 5a-c show representative pull-off strength data obtained from Figures 4a-c by normalizing the force values by the apparent contact area. For spherical probes, the contact area was calculated from the indentation depth (Figure 5d), as was previously done in [2,12,18,19]. The indentation depth itself was calculated from the difference between sample displacement and cantilever deflection. This resulted in graphs where pull-off strength is plotted against preload pressure. In Figure 5b and 5d the same jump in adhesive interaction between probe and AR0.2 sample as in Fig. 4a can be found. While pull-off strength for spherical probes decreased with increasing preload pressure, constant pull-off strength values were found for flat probe measurements.

4. DISCUSSION

4.1. Effect of Tilt Angle on Pull-Off Forces for Flat Probe Measurements

Figure 3 shows that the pull-off force is a function of misalignment and preload if adhesion measurements are performed using a flat probe. The highest pull-off force is found for measurements in the aligned state, and the pull-off force shows little or no preload dependence. A slight preload dependence may be caused by a very small misalignment within the error tolerance, roughness of the sample or dirt particles on the probe and sample. With increasing tilt angle, the pull-off force decreases and becomes more preload dependent. This behavior is to be expected as the probe needs to indent the sample deeper to form complete contact with increasing tilt angle. The increased preload dependence is also a consequence of indentation depth; for low preloads and higher misalignment the flat probe cannot form complete contact with the sample, thus reducing the contact area. Both effects are expected to be dependent on the dimension of the flat probe. Figure 6 schematically shows a contact with perfect alignment (Fig. 6a) and with a misalignment angle θ (Figure 6b).

Interestingly, the drop in adhesion for increasing misalignment is more pronounced for structured samples than for flat ones. In particular, the AR0.2 structures seem to be more sensitive to misalignment

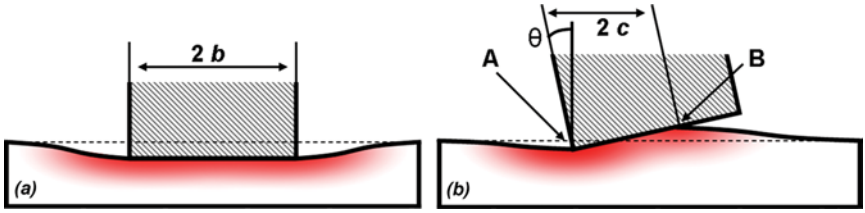

FIGURE 6 Schematic of indentation into a compliant half space with a hard rigid flat probe in (a) the aligned and (b) the misaligned case. (a) Complete contact between probe and sample is formed at low preloads and with small deformation of the sample, resulting in high adhesion and low preload dependence of the pull-off force. (b) Substantial deformation is required to form complete contact, resulting in a preload dependent and reduced pull-off force. The dashed lines represent the half space before deformation (color figure available online).

than AR0.4 structures as shown in Figs. 3b and c. The effect increases with decreasing structure height. Note that the angle sensitivity of the pull-off forces may depend on the pillar tip geometry as well and will be investigated in further studies.

4.2. Effect of Probe Geometry

The adhesion measurements with spherical probes proved that the pull-off force is independent of the alignment, as expected. For AR0.2 structures, an abrupt increase in pull-off force was found at a preload of ~2.5 mN (see Fig. 4a). This increase in pull-off force may be caused by a "break-through" of the probe to the backing layer, which was visualized in earlier studies for low aspect ratio structures [1]. If a spherical probe is pressed into a structured sample, it will form contact with the backing layer at a certain preload. This results in a larger area of contact, increasing the released adhesion energy. However, this "break-through" event is not linked to the indentation depth of the probe. Figure 5d shows that the same indentation depth is reached with the 5 mm radius probe, but no increase in pull-off force occurs. If the pull-off strength is plotted *vs.* preload pressure, however, the jump in pull-off strength occurs at preload pressures which have not been investigated for the 5 mm radius probe in this study.

Figure 7 shows the pull-off forces for structured samples normalized by the values from flat (unstructured) control samples, which allows closer investigation of probe geometry effects. While flat probe measurements result in normalized pull-off force values of ~38% for

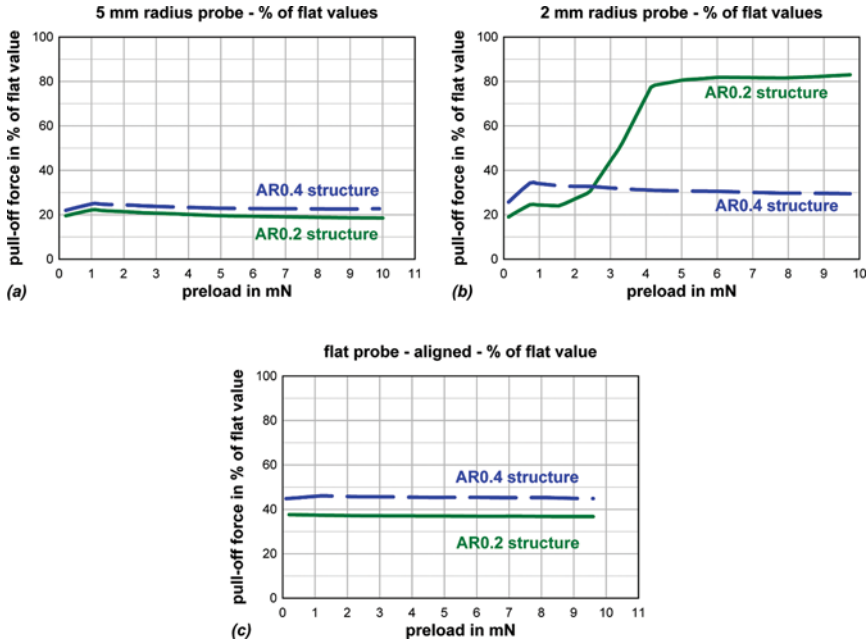

FIGURE 7 Pull-off forces measured on samples with ~0.82 μm (AR0.2 structures) and ~1.95 μm structure height (AR0.4 structures). The pull-off forces were divided by pull-off force values obtained for measurements on flat (unstructured) PDMS. The graphs show results from measurements with (a) flat probes, (b) spherical probes of 2 mm radius, and (c) 5 mm radius (color figure available online).

AR0.2 structures and ~43% for AR0.4 structures (Fig. 7a), measurements with spherical probes lead to lower relative pull-off forces. Relative pull-off force values of ~22% (disregarding the values for preloads larger than 1.5 mN) and ~34% were found for AR0.2 and AR0.4 structures using the 2 mm radius probe (Fig. 7b). Measurements with the 5 mm radius probe resulted in values of ~20% and ~24% (Fig. 7c).

The sensitivity of structured surfaces to misalignment, as mentioned in the previous section, would explain the discrepancy in pull-off force ratios measured for different probe geometries. Due to the curvature of the spherical probe, structures directly under the center of the probe are measured in an aligned state, while structures on the contact periphery will experience a misalignment angle. This misalignment due to probe curvature will result in a lower pull-off force for those structures. This insight leads to two important points: first, experiments with flat aligned probes show results different from

measurements with spherical probes, even if the probe radius is 3 orders of magnitude larger than the structure size; and, second, the adhesive properties of structured samples are rather poor when tested with spherical probes.

Another interesting result is the influence of structure height. Figures 3b and c show that AR0.4 structures have higher pull-off forces than AR0.2 structures. We investigated this now well-known phenomenon in earlier studies [2]. However, while measurements with flat probes and the 5 mm spherical probe show similar ratios of normalized pull-off force values (~1.2 for normalized AR0.4 structured divided by normalized AR0.2 structures, see Figures 7a and c), the ratio calculated for measurements with the 2 mm radius probe is higher (~1.4 in the preload range from 0 to 1.5 mN). This indicates that structures with a higher aspect ratio tend to adhere better to spheres with smaller radii. Structures with higher aspect ratio are easier to bend than those with low aspect ratio and, therefore, do not store as much elastic energy when adapting to misalignment. These results underline the importance of the aspect ratio of the structure for the design of bioinspired adhesive systems.

4.3. Model for the Effect of Misalignment on the Pull-Off Force for a Flat Probe on a Flat Sample

To describe the angle dependence of the pull-off force for flat probes on flat samples we propose the following simplified model. We consider a flat, rigid probe with a square contact area of cross-section $2b \times 2b$, to be adhered to a compliant, isotropic, linear elastic half-space, and analyze the problem in plane strain. A complete edge, A, of the cross section, with length $2b$, forms perfect contact with the substrate as depicted in Fig. 6, while the tilt angle θ is defined as a rotation around A. Let the probe be far away from the sample and then approach it until they touch along A. Adhesive interactions will cause the sample to attach to the probe, and an adhered segment will spontaneously generate along the bottom of the probe, extending $2c$ from A to B (see Fig. 6). If the probe is not permitted to move or rotate, the spontaneous adhesion will cause a tensile load P, and, as in Kendall's problem [39], a square root singularity for stress will appear in the sample at A and B. The stress intensity factors for these singularities at A and B are given by [40]

$$K_I^A = \frac{P}{b\sqrt{\pi c}} - \frac{1}{2}E'\theta\sqrt{\pi c} \tag{1}$$

$$K_I^B = \frac{P}{b\sqrt{\pi c}} + \frac{1}{2}E'\theta\sqrt{\pi c}, \tag{2}$$

where $E' = E/(1-\nu^2)$, with E being the Young's modulus of the sample and ν its Poisson's ratio. Since θ is positive, $K_I^B > K_I^A$.

For equilibrium, the energy release rate at B, given by $(K_I^B)^2/2E'$ [41], must equal the adhesive energy, w, from which we find

$$P = b\left(\sqrt{2\pi E' w c} - \frac{\pi}{2}E'\theta c\right). \tag{3}$$

Since the energy release rate $G^A = \frac{K_I^{A^2}}{2E'}$ at point A is smaller than w, the attachment will attempt to extend around the corner at A and up the side wall of the probe. If the corner is sharp (right angle or very small edge radius) and misalignment is small, the energy release rate will rise very rapidly as the attachment extends due to the severe elastic deformations necessary. As a consequence, the attachment will not extend very far up the side wall of the probe past A. Therefore, we can simply regard the adhesion to terminate at A.

Now consider the misaligned state ($\theta > 0$). If the applied force is zero, the Eq. (3) can be rearranged to predict a value for the half length of the adhesion, c_o, at zero load, namely

$$c_0 = \frac{8w}{\pi E'\theta^2}. \tag{4}$$

If $c_o > b$, the entire bottom surface of the probe will attach. It follows that this will occur when $\theta \le \sqrt{8w/\pi E' b}$, and so very small misalignment, or its absence, will lead to full attachment of the probe at zero load.

Now let the probe attach partially at zero load, so that Eq. (4) is valid for the half length of the attachment. To create an attachment for which the half length is larger than c_o, Eq. (3) indicates that a compressive force is required. Conversely, an attachment having a half length shorter than c_o requires a tensile load to be applied. The form of Eq. (3) makes it obvious that $P = 0$ occurs when $c = 0$. It follows that there is a maximum tensile load for a value of c lying between 0 and c_o; this will be the pull-off load, P_c, found to be

$$P_c = \frac{wb}{\theta}. \tag{5}$$

When $2w/\pi E'\theta^2 < b \le 8w/\pi E'\theta^2$, the probe will be fully adhered at zero load, but the attached length of the adhesion will reduce stably when a small tensile load is applied. This stable process will continue as larger

loads are applied, causing the attached length to reduce, until the applied load equals P_c and the probe detaches. It follows that P_c from Eq. (5) is the pull-off load for all cases, where $\theta > \sqrt{2w/\pi E' b}$.

Now, consider cases where $\theta \leq \sqrt{2w/\pi E' b}$. The probe will be fully attached at zero load, but with shrinking attachment length the applied load will diminish. It follows that as soon as a sufficiently high load is applied to cause the attached length to shrink, the probe will detach unstably. The detachment process will commence when the energy release rate at point B equals the adhesion energy. It follows that in this situation the pull-off load will be given by Eq. (3) with c replaced by b. The complete picture is given by

$$\begin{aligned} P_c &= b\left(\sqrt{2\pi E' w b} - \frac{\pi}{2} E' \theta b\right) \quad \theta \leq \sqrt{\frac{2w}{\pi E' b}} \\ P_c &= \frac{bw}{\theta} \qquad\qquad\qquad\qquad \theta > \sqrt{\frac{2w}{\pi E' b}}. \end{aligned} \tag{6}$$

4.4. Comparison with Data in Figure 3

If we take the second of the predictions in Eq. (6), valid for larger misalignment, we deduce that the experimental results for the asymptotic

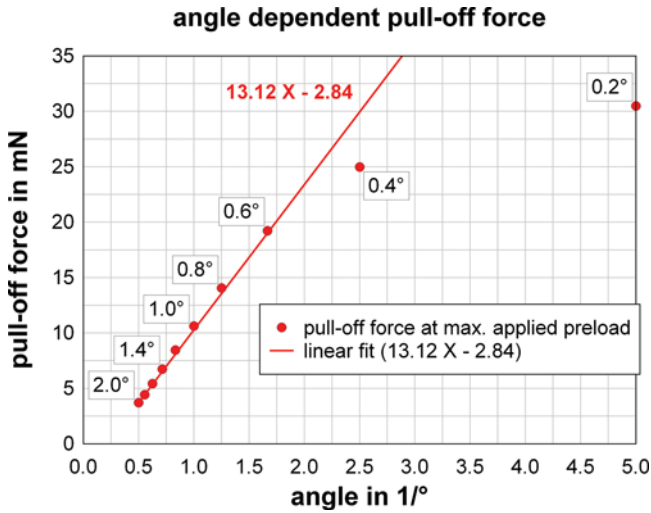

FIGURE 8 Pull-off force at maximum preload versus the inverse tilt angle. A linear fit is drawn for tilt angles larger than 0.4° with a slope of 13.12 mN° and a y-axis intercept of −2.84 mN (color figure available online).

behavior for large preload should be inversely proportional to the misalignment angle. In Fig. 8 the pull-off force at maximum applied preload ($\sim$10 mN) is plotted *versus* the inverse tilt angle.

As predicted, the pull-off force is proportional to $1/\theta$, restricted to tilt angles larger than 0.4°. According to Eq. (5) the slope of the fit is proportional to the adhesion energy, computed to be $0.46\,J/m^2$, where we have used the probe radius of 0.5 mm as the value for b. According to the model, the y-axis intercept of the linear fit should be zero. The offset apparent in Fig. 8 may arise for several reasons, ranging from experimental errors due to the small preloads applied, to friction effects that cannot be controlled. In addition, the model presented is based on plane strain calculations, while the results shown in Figure 3a are for a three-dimensional configuration, introducing further imprecision in the comparison of the model with the experimental results.

5. SUMMARY

In this study, we compared adhesion measurements on flat and structured samples using different probe geometries, namely flat probes and spherical probes with 2 and 5 mm radii. The following conclusions can be drawn:

- Adhesion measurements with flat probes strongly depend on the misalignment angle. For measurements in an aligned configuration there is little or no preload dependence of the pull-off forces. Increasing misalignment causes a significant drop in pull-off force and increases its preload dependence.
- Pillar structures are more sensitive to misalignment than flat control samples, if tested with a flat probe. This behavior may differ with varying tip geometry and aspect ratio of the structures.
- Adhesion measurements with spherical probes are independent of alignment. Tilting the probe $+/-2°$ does not influence the pull-off force.
- The ratio of pull-off force measured for structured samples to that for flat samples depends on the probe geometry. Measurements with spherical probes lead to lower values of pull-off forces for structured samples due to their curvature-dependent misalignment.
- Experiments with flat aligned probes show an adhesion behavior different from those obtained with a spherical probe, even if the radius of the spherical probe is 3 orders of magnitude larger than the structure features.

- For the spherical probe with 2 mm radius, a jump in pull-off force was observed, which may be caused by a "breakthrough" to the backing layer. This effect is not linked to indentation depth by the probe but may be a function of preload pressure, structure aspect ratio and structure spacing.
- Aligned flat probes do not experience a variation in their contact area, thus resulting in preload independent pull-off strength values, allowing a straight-forward evaluation of adhesion performance.
- We have proposed a simple model describing the effect of probe tilting on the pull-off forces at high preloads.

Spherical probes involve a simple experimental setup; however, aligned flat probes lead to direct acquisition of the pull-off strength, which is of significance in the evaluation of adhesive properties in an engineering context. Furthermore, effects such as the tilt angle dependence of adhesion for structured samples can be quantified, or—in the case of measurements in the aligned configuration—avoided.

Supporting Information Available: Additional graphs of tilt dependent pull-off force measurements for 2 and 5 mm radius spherical probes and a flat probe are shown.

The authors thank Joachim Blau for his ideas for improving the adhesion tester, Marleen Kamperman for inspiring discussions, Thomas Nauhauser for his helping hand in several experiments, and all members of the Functional Surfaces Group at the INM–Leibniz-Institute for New Materials for fruitful collaboration. This work was funded by Volkswagen-Stiftung.

ACKNOWLEDGMENTS

The authors thank Joachim Blau for his ideas for improving the adhesion tester, Marleen Kamperman for inspiring discussions, Thomas Nauhauser for his helping hand in several experiments, and all members of the Functional Surfaces Group at the INM – Leibniz Institute for New Materials for fruitful collaboration. This work was funded by Volkswagen-Stiftung.

REFERENCES

[1] Crosby, A. J., Hageman, M., and Duncan, A., *Langmuir* **21**, 11738–11743 (2005).
[2] Greiner, C., del Campo, A., and Arzt, E., *Langmuir* **23**, 3495–3502 (2007).

[3] Majidi, C., Groff, R. E., Maeno, Y., Schubert, B., Baek, S., Bush, B., Maboudian, R., Gravish, N., Wilkinson, M., Autumn, K., and Fearing, R. S., *Phys. Rev. Lett.* **97**, 076103 (2006).
[4] Peressadko, A. and Gorb, S., *J. Adhes.* **80**, 1–15 (2004).
[5] Varenberg, M., Peressadko, A., Gorb, S., and Arzt, E., *Appl. Phys. Lett.* **89**, 121905 (2006).
[6] Glassmaker, N. J., Jagota, A., Hui, C.-Y., Noderer, W. L., and Chaudhury, M. K., *Proc. Natl. Acad. Sci. USA.* **104**, 10786 (2007).
[7] Greiner, C., Arzt, E., and del Campo, A., *Adv. Mater.* **21**, 479–482 (2009).
[8] Jeong, H. E., Lee, J.-K., Kim, H. N., Moon, S. H., and Suh, K. Y., *Proc. Nat. Acad. Sci.* **106**, 5639–5644 (2009).
[9] Lee, J., Bush, B., Maboudian, R., and Fearing, R. S., *Langmuir* **25**, 12449–12453 (2009).
[10] Murphy, M. P., Kim, S., and Sitti, M., *Appl. Mater. Interface* **1**, 489–855 (2009).
[11] Vajpayee, S., Long, R., Shen, L., Jagota, A., and Hui, C.-Y., *Langmuir* **25**, 2765–2771 (2009).
[12] Aksak, B., Murphy, M. P., and Sitti, M., *Langmuir* **23**, 3322–3332 (2007).
[13] Murphy, M. P., Aksak, B., and Sitti, M. J., *Adhes. Sci. Technol.* **21**, 1281–1296 (2007).
[14] Murphy, M. P., Aksak, B., and Sitti, M., *Small* **5**, 170–175 (2009).
[15] Davies, J., Haq, S., Hawke, T., and Sargent, J. P., *Int. J. Adhes. Adhes.* **29**, 380–390 (2009).
[16] del Campo, A., Álvarez, I., Filipe, S., and Wilhelm M., *Adv. Funct. Mater.* **17**, 3590–3597 (2007).
[17] del Campo, A., Greiner, C., Álvarez, I., and Arzt, E., *Adv. Mater.* **19**, 1973–1977 (2007).
[18] del Campo, A., Greiner, C., and Arzt, E., *Langmuir* **23**, 10235–10243 (2007).
[19] Gorb, S., Varenberg, M., Peressadko, A., and Tuma, J., *J. R. Soc. Interface* **4**, 271–275 (2007).
[20] Kim, S., Aksak, B., and Sitti, M., *Appl. Phys. Lett.* **91**, 221913 (2007).
[21] Kim, S. and Sitti, M., *Appl. Phys. Lett.* **89**, 261911 (2006).
[22] Santos, D., Spenko, M., Parness, A., Kim, S., and Cutkosky, M. J., *Adhes. Sci. Technol.* **21**, 1317–1341 (2007).
[23] Kim, T., Jeong, H. E., Suh, K. Y., and Lee, H. H., *Adv. Mater.* **21**, 2276–2281 (2009).
[24] Kim, S., Sitti, M., Xie, T., and Xiao, X., *Soft Matter* **5**, 3689–3693 (2009).
[25] Reddy, S., Arzt, E., and del Campo, A., *Adv. Mater.* **19**, 3833–3837 (2007).
[26] Johnson, K. L., Kendall, K., and Roberts, A. D., *Proc. R. Soc. Lond. Ser. A.* **324**, 301–313 (1971).
[27] Kendall, K. Ph.D. dissertation, "The Stiffness of Surfaces in Static and sliding Contact", Cambridge University (UK) (1969).
[28] Roberts, A. D. Ph.D. dissertation, "The Extrusion of Liquids between Highly Elastic Solids", Cambridge University (UK) (1968).
[29] Derjaguin, B. V., Muller, V. M., and Toporov, Y. P. J., *Colloid Interface Sci.* **53**, 314–326 (1975).
[30] Greiner, C., Spolenak, R., and Arzt, E., *Acta Biomater.* **5**, 597–606 (2009).
[31] Hertz, H. J., *Reine angew. Math.* **92**, 156–171 (1881).
[32] Kim, K. S., McMeeking, R. M., and Johnson, K. L., *J. Mech. Phys. Solids* **46**, 243 (1998).
[33] Maugis, D. J., *Colloid Interface Sci.* **150**, 243 (1992).
[34] Schargott, M., Popov, V. L., and Gorb, S. J., *Theor. Biol.* **243**, 48–53 (2006).

[35] Spolenak, R., Gorb, S., Gao, H. J., and Arzt, E., *Proc. R. Soc. London, Ser. A* **461**, 305–318 (2004).
[36] Tabor, D. J., *Colloid Interface Sci.* **58**, 2–13 (1977).
[37] Kroner, E., Maboudian, R. and Arzt, E., *Adv. Eng. Mater.* **12**, 398–404 (2010).
[38] Kroner, E., Blau, J., and Arzt, E., to be published
[39] Kendall, K. J., *Adhes.* **5**, 77–79 (1973).
[40] Tada, H., Paris, P. C., and Irwin, G. R., *The Stress Analysis of Cracks Handbook*, (Del Research Corporation, Hellertown, PA, USA, 1973), 3rd Ed.
[41] Johnson, K. L., *Contact Mechanics*, (Cambridge University Press, Cambridge, UK, 1987), 9th Ed.

SUPPORTING INFORMATION

The following figures show all adhesion measurements presented in the paper as a 2.5 dimensional graph. The x-axis shows the measurement angle, the y-axis the preload and the pull-off force is color coded. The headline of each graph indicates the measurement system (probe geometry on sample geometry). AR0.2 indicates the structures with approx. 0.82 μm and AR0.4 samples with approx. 1.95 μm height. All structure diameters were approx. 4.7 μm, hexagonally packed with a spacing of approx. 5 μm in between the structures.